Self-Assembled Pb Nanostructures on Si(111) Surfaces: From Nanowires to Nanorings

By *Rui Wu, Yi Zhang, Feng Pan, Li-Li Wang, Xu-Cun Ma,* Jin-Feng Jia,* and *Qi-Kun Xue**

A template-directed growth method for metals is described in which ordered arrays of super-long single-crystalline metal nanowires with atomic-level-controlled width, thickness (height), and surface location are prepared by molecular beam epitaxy. Their subsequent examination by in situ scanning tunneling microscopy is also outlined. A phase-separated stripe pattern composed of alternately a Ge-rich incommensurate phase and a $\sqrt{3}\times\sqrt{3}$ phase is first obtained by Ge deposition on Si(111) substrates. Further deposition of Pb on this patterned surface leads to a well-ordered array of super-long Pb nanowires. Using the same mechanism, superconducting Pb nanorings can also be fabricated. In this review of our recent work, these Pb single-crystalline nanowires and nanorings are shown to serve as an ideal platform for the study of superconductivity in reduced dimensionalities. Furthermore, because the widths and spatial distributions of two phases can be precisely controlled by the Ge coverage and substrate temperature, and because a metal will always selectively nucleate on one of two phases, this template-directed growth method can be applied to a wide range of metals.

1. Introduction

Low-dimensional nanostructures exhibit quantum confinement effects and exotic electronic, optical, and magnetic properties, which can be exploited to develop novel nanometer-scale electronic and optoelectronic devices.[1] In this regard, fabrication of one-dimensional (1D) nanowires and nanorings and their assembly into ordered arrays is of particular interest and has been extensively investigated in the last three decades.[2] In order to prepare metal nanowires and nanorings with diameters in the sub-100 nm range, three approaches have usually been used: lithography,[3a,b] template-directed growth,[3c,d] and self-assembly in chemical synthesis[3e,f]/strain-mediated expitaxy.[3g] Of these approaches, growth by template-directed molecular beam epitaxy (MBE) has recently shown great promise for preparing macro-long (up to millimeter scale) metal nanowires while their diameters and locations on a substrate surface can be simultaneously and precisely controlled on the nanometer scale.[4] However, for nanorings, atomic-scale control of their size remains a daunting challenge in the existing self-assembly methods.

This Research News reports a detailed scanning tunneling microscopy (STM) study of Ge-induced phase-separated surfaces on Si(111) and further Pb nanostructure growth on them. By selection of the proper substrate temperature and terrace width, phase-separated stripe and island structures were obtained, both of which are characterized by an alternate distribution of the Ge-induced incommensurate phase and the $(\sqrt{3}\times\sqrt{3})$ R30° phase (called $\sqrt{3}\times\sqrt{3}$ hereafter). More importantly, in terms of different surface reactivities of the two phases, the expected template effect of the phase-separated surfaces is verified by self-assembled arrays of Pb nanowires with atomic-level-controlled width and thickness (height) and nanorings on stripe and island structures, respectively. A discussion of the various applications and opportunities of such self-assembled nanostructures is presented.

2. Growth of Ge-Induced Phase-Separated Surfaces on Si(111)

The Ge-rich incommensurate phase coexists with the $\sqrt{3}\times\sqrt{3}$ phase on Si(111)-(7×7) surfaces covered with between 1/3 monolayer (ML) and 1 ML. Under proper experimental conditions, the incommensurate phase forms along the lower edge of a Si step and the $\sqrt{3}\times\sqrt{3}$ phase along the upper edge of the Si step, which can result in a phase-separated stripe structure on each terrace of the Si substrate. Phase-separated islands are also obtained, depending on the substrate temperature and the Si terrace width.

2.1. Phase-Separated Stripe Surface: Coverage-Dependent Surface Structures

The experiments were performed in an MBE system combined with an ultrahigh vacuum (ca. 2×10^{-10} mbar (1 mbar = 100 Pa))

[*] Prof. X.-C. Ma, R. Wu, Y. Zhang, Dr. L.-L. Wang
State Key Laboratory for Surface Physics
Institute of Physics, Chinese Academy of Sciences
Beijing 100190 (P. R. China)
E-mail: xcma@aphy.iphy.ac.cn
Prof. Q.-K. Xue, Dr. F. Pan, Prof. J.-F. Jia
Department of Physics, Tsinghua University
Beijing 100084 (P. R. China)
E-mail: qkxue@mail.tsinghua.edu.cn

DOI: 10.1002/adma.200901063

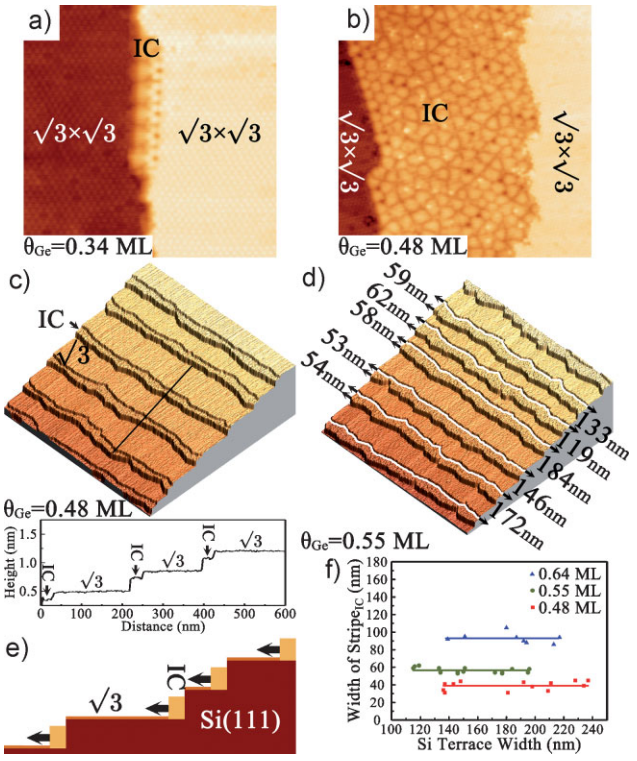

Figure 1. a–d) STM images showing surface morphologies after deposition of different amounts of Ge on Si(111) surfaces with an average terrace width of ca. 180 nm at 550 °C. Coverages: a) 0.34 ML, b) 0.48 ML, c) 0.48 ML (3D view), and d) 0.55 ML (3D view). In (c), the line profile corresponding to the black line is shown at the bottom. In (d), every Si step edge is marked by a white line, and the Si terrace width and the incommensurate stripe width are indicated. All images were acquired at a sample bias of +3 V. Image sizes: a) 30 nm × 30 nm, b) 50 nm × 50 nm, and c,d) 1000 nm × 1000 nm. e) Schematic diagram of Ge-induced stripe surface on Si(111). f) Incommensurate stripe width versus Si terrace width for different amounts of Ge.

variable-temperature scanning tunneling microscope. Si(111) substrates with a nominal terrace width of ca. 180 nm were used. Ge (99.999%) was evaporated onto the Si(111)-(7 × 7) surfaces at a typical flux rate of 0.05 ML min^{-1} (1 ML = 7.8×10^{-14} atoms cm^{-2}), while the substrates were kept at 550 °C. All of the STM images were taken at room temperature with a tunneling current of 0.02 nA.

The STM images in Figures 1a–d display the surface morphologies after the deposition of different amounts of Ge on Si(111) substrates. At $\theta_{Ge} = 0.34$ ML, which is slightly greater than 1/3 ML of the $\sqrt{3} \times \sqrt{3}$ phase[5] (Fig. 1a), the Ge-rich incommensurate phase starts to nucleate at the Si step edges. With increasing Ge coverage, the incommensurate phase grows towards the terrace and along the step (Fig. 1b). At $\theta_{Ge} = 0.48$ ML (Fig. 1c), a stripe of the incommensurate phase with a width of 39 ± 7 nm forms on every Si terrace. More interestingly, the stripes run the whole length of the step on the substrate. Depending on the size of the Si sample used, the length of the stripes can reach the millimeter scale and even longer. This is the most important feature of the striped surface morphology.

Once the incommensurate stripes stretch from one end of the step to the other, further increase of the Ge coverage allows the stripes grow laterally. Note that the substrate in Figure 1d ($\theta_{Ge} = 0.55$ ML) exhibits different terrace widths, 119, 133, 146, 172, and 184 nm. However, the incommensurate stripes all have a width of 57 ± 5 nm, for example, 62, 59, 53, 54, and 58 nm. As shown in Figure 1f, despite one terrace being almost twice the width of another, the corresponding incommensurate stripes remain the same widths: 39 ± 7 nm for $\theta_{Ge} = 0.48$ ML, 57 ± 5 nm for $\theta_{Ge} = 0.55$ ML, and 94 ± 10 nm for $\theta_{Ge} = 0.64$ ML. That is, for a given Si substrate, the resulting width of the incommensurate stripes is independent of the substrate terrace size and depends only on the Ge coverage. This is the second unique feature of the Ge-induced stripe surface.

By the line profile measurement in Figure 1c, we studied the formation mechanism of the striped surfaces. We note that the electronic density of states near the Fermi energy in the Ge-rich incommensurate phase is higher than in $\sqrt{3} \times \sqrt{3}$. In an STM image, the incommensurate phase should look brighter than $\sqrt{3} \times \sqrt{3}$. The Si terrace step is 0.31 ± 0.01 nm; the apparent height difference between the incommensurate phase and $\sqrt{3} \times \sqrt{3}$ is 0.21 ± 0.02 nm when the two phases are on the same terrace and 0.11 ± 0.02 nm when they are on neighboring terraces. This result suggests that the incommensurate phase always nucleates at the lower edge of a step and grows towards the terrace center, provided that the incommensurate phase grows at the expense of any $\sqrt{3} \times \sqrt{3}$ that might form first and the Ehrlich-Schwoebel barrier[6a,6b] for down-step diffusion of Ge atoms on the $\sqrt{3} \times \sqrt{3}$ surface might be very small.[6c] At a substrate temperature of 550 °C, the Ge atoms should migrate "freely" on the terrace and be able to cross step edges. The fact that the incommensurate stripes have the same width supports the assumption of the nearly barrier-free diffusion of Ge atoms between different terraces. Otherwise, the width of the incommensurate stripe on a wider Si terrace should be greater because more Ge atoms have arrived on the terrace. To summarize, the formation of the incommensurate phase is facilitated by nucleation at the lower edge of a step and propagation to the terrace center by a step-flow mode,[7] as schematically illustrated in Figure 1e.

By statistical analysis with different Si substrates and Ge coverages (see Fig. 1f), we were able to find a quantitative empirical relationship between the Ge coverage and the width of the incommensurate stripes. The Ge coverage θ_{Ge} deposited on Si(111) can be expressed by

$$\theta_{Ge} = \theta_{inc} W_{inc} \sum_{i=1}^{n} L_i + \theta_{\sqrt{3}} \left(1 - W_{inc} \sum_{i=1}^{n} L_i \right) \quad (1)$$

where θ_{inc} and $\theta_{\sqrt{3}}$ are the coverage of the incommensurate phase and the $\sqrt{3} \times \sqrt{3}$ phase, respectively, W_{inc} is the width of the incommensurate stripe, L_i the length of the ith Si step, and n the number of Si terraces. Define $C_{Si} = \sum_{i=1}^{n} L_i$, which reflects the step density determined by the cutting angle of a Si wafer. We obtain

$$W_{inc} = \frac{1}{C_{Si}} \cdot \frac{\theta_{Ge} - \theta_{\sqrt{3}}}{\theta_{inc} - \theta_{\sqrt{3}}} \quad (2)$$

Therefore, the Ge coverage and the step density are the only two factors that determine the incommensurate stripe width, provided the Ge coverage lies in the range 1/3 ML to 1 ML and the temperature is high enough to allow sufficient Ge diffusion on the $\sqrt{3} \times \sqrt{3}$ surface. One can precisely control the incommensurate stripe width by the Ge coverage or the cutting angle of the Si wafer. Clearly, the experiment demonstrates a simple and practical way to fabricate a tunable template with remarkable control of its structure.

2.2. Phase-Separated Islands: Temperature- and Terrace-Width-Dependent Surface Structures

As mentioned above, in order to prepare the phase-separated stripe surfaces, the substrate temperature must be high enough to ensure sufficient Ge diffusion. When the substrate temperature is slightly lower and the terrace width becomes larger, another interesting structure—phase-separated islands—is observed. As we shall see in Section 3, such islands can be used as a template for growth of nanorings.

Figure 2a displays an STM image of the Si substrate deposited with 0.40 ML Ge at 470 °C. The central terrace in the image is ca. 800 nm wide. In addition to the incommensurate stripes along the Si steps, there are also four islands with two different contrasts on the terrace. The high resolution STM image (Fig. 2b) of one of the islands reveals that the island center is the $\sqrt{3} \times \sqrt{3}$ phase, surrounded by the incommensurate phase, which forms a hollow hexagon ring-like structure. From the line profile in the lower panel of Figure 2a, two horizontal dashed lines indicate that the central and surrounding parts have the same heights as the striped $\sqrt{3} \times \sqrt{3}$ phase on the upper terrace and incommensurate phase on the same terrace, respectively. We speculate that the inner part of the island is most likely a newly grown Si layer due to limited atom diffusion. If this is the case, formation of the ring-like structure is not surprising, since the edge of this new island can serve as a nucleation center for the incommensurate phase in the same way as the steps discussed above.

We studied more than 50 islands from different surface locations. The phase-separated islands are only formed on terraces wider than ca. 700 nm at a Ge coverage of 0.4 ML and a substrate temperature of 470 °C (see Fig. 2c). Also, the islands could not be formed by Ge deposition on Si(111) substrates with a terrace width of either ca. 860 nm at 550 °C or ca. 180 nm at 470 °C. Thus, we can state that some Ge atoms that can diffuse "freely" near step edges collect to form incommensurate stripes, while some Ge atoms on larger terraces aggregate to form phase-separated islands, which depend on both the substrate temperature and the terrace width.

3. Growth of Pb Nanowires and Nanorings

The $\sqrt{3} \times \sqrt{3}$ phase and the incommensurate phase have different atomic and electronic structures.[8] Given that a metal does not react strongly with the substrate and can diffuse, preferential adsorption and growth of the metal on one of the two phases should be expected to occur on the surfaces with stripes and islands. In this context, the Ge-decorated surfaces may be an ideal template to direct nanostructure growth. Here, we choose Pb to examine the possible template effect of the phase-separated surfaces. Pb is also a group IV element and does not react with Ge or Si. Deposition of Pb on the Si or Ge substrate usually leads to a very sharp interface.[1a,9]

3.1. Pb Nanowires on a Surface with Phase-Separated Stripes

Pb (99.999%) was evaporated onto the Ge/Si substrates at a typical flux rate of 0.18 ML min^{-1}, while the substrates were cooled down to ca. 150 K. STM observations were performed after the samples had been gradually warmed up to room temperature. Figure 3a shows an STM image after ca. 3.6 ML Pb was deposited on the

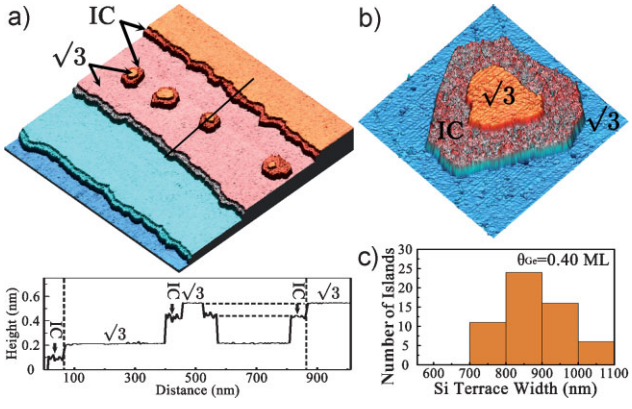

Figure 2. a,b) 3D-view STM images of 0.40 ML Ge deposited on a Si substrate with an average terrace width of ca. 860 nm at 470 °C. In (a), the line profile corresponding to the black line is shown at the bottom. Both images were acquired at a sample bias of +3 V. Image sizes: a) 2000 nm × 2000 nm, and b) 200 nm × 200 nm. c) Statistical histogram of numbers of islands versus Si terrace width.

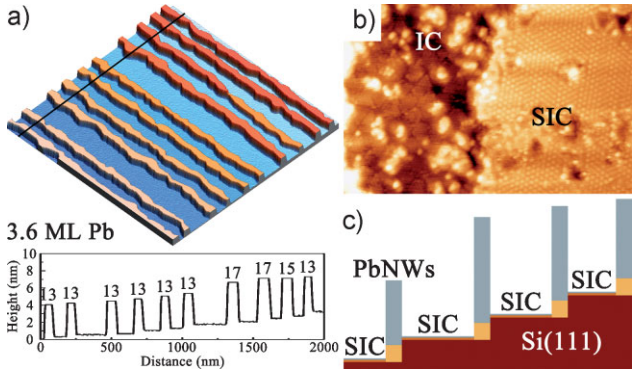

Figure 3. a) 3D-view STM image showing a highly ordered array of nanowires after 3.6 ML Pb was deposited on the striped surface. The line profile corresponding to the black line is shown at the bottom. b) High-resolution STM image of the exposed substrate surface after some of the Pb nanowires were removed by the STM tip. The sample biases are −4.5 V in (a) and +1.5 V in (b). Image sizes: a) 2000 nm × 2000 nm and b) 30 nm × 45.6 nm. c) Schematic diagram showing the formation mechanism of nanowire arrays on the surface with Ge-induced stripes.

striped surface (Fig. 1d), where a highly ordered array of nanowires is immediately evident. The width of the wires, as measured by the line profile, is 55 ± 10 nm, which is consistent with that of the incommensurate stripes (57 ± 5 nm) and suggests that Pb grows exclusively on top of the Ge-rich incommensurate phase. To confirm this, we performed high-bias STM scans of a certain region. Due to tip-induced atom diffusion at high bias (−4.5 V), some of the Pb nanowires can be successfully removed. The high-resolution STM image of the exposed substrate surface (Fig. 3b) indicates that the Pb nanowires are indeed formed on top of the incommensurate phase, and the original $\sqrt{3} \times \sqrt{3}$ phase transforms into a striped incommensurate (SIC) phase by intermixing of Pb and Ge adatoms, which is similar to the SIC phase of the Pb/Si(111) system.[10] The selective growth lies in the fact that the incommensurate phase has minimal lattice mismatch with the Pb(111)–1×1 surface, compared to $\sqrt{3} \times \sqrt{3}$. Based on these observations, we propose a model for the nanowire growth, as schematically illustrated in Figure 3c. According to this model, for a given Si substrate, the width of the Pb nanowires can be steadily controlled since the Ge coverage is the only factor that determines the width of the incommensurate stripes.

In the selected growth mode, control of another dimension of the Pb nanowires, the thickness (height), becomes straightforward. Assuming that all deposited Pb atoms are incorporated into the substrate without desorption, one can easily imagine that the only factor that determines thickness is the Pb coverage. As shown in the line profile (Fig. 3a), the nanowires have a dominant thickness of 13 ML, and some nanowires of 15 ML and 17 ML appear near wider terraces. This fluctuation is largely due to the inhomogeneity of the Si substrate. It is not surprising since the wider terraces collect more Pb atoms and the nanowires formed nearby should be thicker. Another reason for the observed thickness fluctuation is the quantum size effects in Pb.[1a,3g,4] 15 ML and 17 ML are the thicknesses favored by quantum size effects. Although 14 ML is the next thickness to grow, wires at this thickness are not energetically stable and thus cannot form. The situation can be improved if the Si substrate is properly treated and has more uniform terraces. Consequently, producing an ordered array of super-long Pb nanowires with more uniform thickness should not be difficult.

3.2. Pb Nanorings on Phase-Separated Islands

Pb nanorings grow by the same mechanism as the nanowires. In Figure 4a, we show an STM image obtained from a surface with islands (Fig. 2a), on which was deposited ca. 2.7 ML Pb; a ring-like structure appears at the center of the image. The inside diameter, outside diameter, width, and thickness of the ring are 70, 136, 33, and 2.86 nm (10 ML), respectively. Since Pb rings form exclusively on the incommensurate phase of the islands, their sizes can be controlled to a certain extent in the same way as the prepared islands, as discussed in Section 2. We must point out that precise control is more difficult than for the nanowires. The reason is simple: nucleation on a terrace is by nature a random process. As shown in Figures 4b and c, nanorings with different sizes and appearances are formed on different surface regions. Nevertheless, this work represents great progress in preparing nano- and mesorings, which have been demonstrated to be extremely difficult to prepare by the existing growth methods.

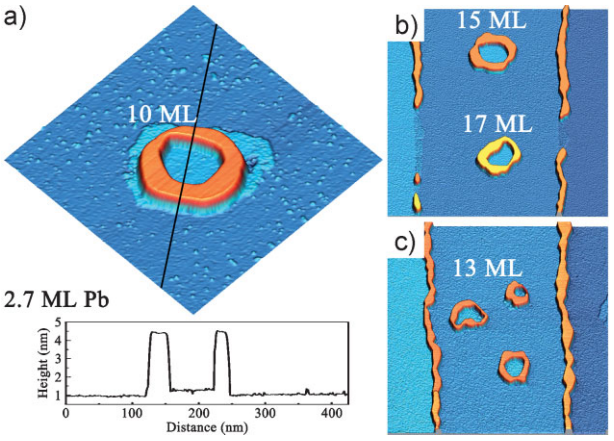

Figure 4. a–c) 3D-view STM images showing Pb nanorings after 2.7 ML Pb was deposited on the island-patterned surface. In (a), the line profile corresponding to the black line is shown at the bottom. All images were acquired at a sample bias of −5 V. Image sizes: a) 350 nm × 350 nm, b) 1200 nm × 1200 nm, and c) 1500 nm × 1500 nm.

4. Conclusion and Outlook

In addition to their novel structures, the single-crystalline Pb nanowires and nanorings reported in this study provide ideal systems for study of quantum phenomena associated with strong 1D confinement, simply because the thickness and width are both comparable to the Fermi wavelength of Pb (1.06 nm). For example, the typical wires shown in Figure 3a are 3.72 nm (13 ML) thick and 58 nm wide, and the equivalent cross section is about 15 nm × 15 nm, which is comparable to the Bardeen–Cooper–Schrieffer (BCS) coherence length (90.5 nm) of bulk Pb at 0 K and the coherence length (27 nm) of Pb thin films.[3b] This suggests it will be an intriguing 1D superconducting system.[11] The fact that the wires have macro-lengths of up to several millimeters makes measurement of their electrical transport properties easier — without the difficulty of fabricating contact electrodes and nanometer-scale positioning — than for the short nanowires that are usually available. In the case of Pb nanorings, many interesting problems, such as the Aharonov–Bohm effect[12a] and persistent current,[12b] can be investigated with the "1D" superconducting rings.[11b,12c]

Surfaces with Ge-induced phase-separated stripes and islands are good templates for the self-assembled growth of nanowires and nanorings, respectively. The method is not necessarily limited to a metal like Pb. It can be extended to other metals, such as Sn, Ga, and In, as long as the metal deposition does not destroy the Ge-induced structures. Moreover, the metal nanostructures prepared on the Ge-decorated substrate can further be used as a new template for growth of similar nanostructures with other materials, and even for growth of lateral superlattices. Gas molecule exposure to these highly ordered nanostructures, if they can indeed be made, would also be expected to afford more

opportunities in self-assembled growth of nanostructures for optical and optoelectronic applications.

Acknowledgements

This work is financially supported by the National Natural Science Foundation and the Ministry of Science and Technology of China.

Published online:

[1] a) Y. Guo, Y. F. Zhang, X. Y. Bao, T. Z. Han, Z. Tang, L. X. Zhang, W. G. Zhu, E. G. Wang, Q. Niu, Z. Q. Qiu, J. F. Jia, Z. X. Zhao, Q. K. Xue, *Science* **2004**, *306*, 1915. b) X. Michalet, F. F. Pinaud, L. A. Bentolila, J. M. Tsay, S. Doose, J. J. Li, G. Sundaresan, A. M. Wu, S. S. Gambhir, S. Weiss, *Science* **2005**, *307*, 538. c) J. Xiang, W. Lu, Y. Hu, Y. Wu, H. Yan, C. M. Lieber, *Nature* **2006**, *441*, 489.

[2] a) R. J. Warburton, C. Schäflein, D. Haft, F. Bickel, A. Lorke, K. Karrai, J. M. Garcia, W. Schoenfeld, P. M. Petroff, *Nature* **2000**, *405*, 926. b) N. A. Melosh, A. Boukai, F. Diana, B. Gerardot, A. Badolato, P. M. Petroff, J. R. Heath, *Science* **2003**, *300*, 112.

[3] a) A. Kosiorek, W. Kandulski, H. Glaczynska, M. Giersig, *Small* **2005**, *1*, 439. b) J. Wang, X. Ma, L. Lu, A. Jin, C. Gu, X. C. Xie, J. Jia, X. Chen, Q. Xue, *Appl. Phys. Lett.* **2008**, *92*, 233119. c) K. L. Hobbs, P. R. Larson, G. D. Lian, J. C. Keay, M. B. Johnson, *Nano Lett.* **2004**, *4*, 167. d) K. Xu, J. R. Heath, *Nano Lett.* **2008**, *8*, 136. e) N. R. Jana, L. Gearheart, C. J. Murphy, *Chem. Commun.* **2001**, 617. f) Y. Sun, Y. Xia, *Adv. Mater.* **2003**, *15*, 695. g) L. L. Wang, X. C. Ma, P. Jiang, Y. S. Fu, S. H. Ji, J. F. Jia, Q. K. Xue, *Phys. Rev. B* **2006**, *74*, 073404.

[4] Z. L. Guan, R. Wu, Y. X. Ning, C. L. Song, L. Tang, D. Hao, X. C. Ma, J. F. Jia, X. Chen, Q. K. Xue, Z. M. Liao, D.-P. Yu, *Appl. Phys. Lett.* **2008**, *93*, 023115.

[5] Z. H. Qin, D. X. Shi, H. F. Ma, H. J. Gao, A. S. Rao, S. Wang, S. T. Pantelides, *Phys. Rev. B* **2007**, *75*, 085313.

[6] a) G. Ehrlich, F. G. Hudda, *J. Chem. Phys.* **1966**, *44*, 1039. b) R. L. Schwoebel, E. J. Shipsey, *J. Appl. Phys.* **1966**, *37*, 3682. c) Morphological Organization in Epitaxial Growth and Removal, (Eds: Z. Y. Zhang, M. G. Lagally), *Ser. Directions in Condensed Matter Physics*, Vol. *14*, World Scientific, Singapore **1998**.

[7] a) B. Voigtländer, T. Weber, P. Šmilauer, D. E. Wolf, *Phys. Rev. Lett.* **1997**, *78*, 2164. b) M. Kawamura, N. Paul, V. Cherepanov, B. Voigtländer, *Phys. Rev. Lett.* **2003**, *91*, 096102.

[8] M. Y. Lai, Y. L. Wang, *Phys. Rev. B* **1999**, *60*, 1764.

[9] J. A. Carlisle, T. Miller, T. C. Chiang, *Phys. Rev. B* **1993**, *47*, 3790.

[10] L. Seehofer, G. Falkenberg, D. Daboul, R. L. Johnson, *Phys. Rev. B* **1995**, *51*, 13503.

[11] a) M. Zgirski, K. Riikonen, V. Touboltsev, K. Arutyunov, *Nano Lett.* **2005**, *5*, 1029. b) K. Y. Arutyunova, D. S. Golubevc, A. D. Zaikin, *Phys. Rep.* **2008**, *464*, 1.

[12] a) Y. Aharonov, D. Bohm, *Phys. Rev.* **1959**, *115*, 485. b) M. Büttiker, Y. Imry, R. Landauer, *Phys. Lett. A* **1983**, *96*, 365. c) F. Loder, A. P. Kampf, T. Kopp, J. Mannhart, C. W. Schneider, Y. S. Barash, *Nat. Phys.* **2008**, *4*, 112.